RSC Advances

PAPER

Cite this: *RSC Adv.*, 2016, **6**, 110466

Self-assembly of water molecules using graphene nanoresonators

Cuixia Wang,[e] Chao Zhang,[ef] Jin-Wu Jiang,[c] Ning Wei,[f] Harold S. Park*[d] and Timon Rabczuk*[abe]

Received 8th September 2016
Accepted 11th November 2016

DOI: 10.1039/c6ra22475j

www.rsc.org/advances

Inspired by macroscale self-assembly using the higher order resonant modes of Chladni plates, we use classical molecular dynamics to investigate the self-assembly of water molecules using graphene nanoresonators. We find that water molecules can assemble into water chains and that the location of the assembled water chain can be controlled through the resonant frequency. More specifically, water molecules assemble at the location of maximum amplitude if the resonant frequency is lower than a critical value. Otherwise, the assembly occurs near the nodes of the resonator provided the resonant frequency is higher than the critical value. We provide an analytic formula for the critical resonant frequency based on the interaction between water molecules and graphene. Furthermore, we demonstrate that the water chains assembled by the graphene nanoresonators have some universal properties including a stable value for the number of hydrogen bonds.

Graphene is a monolayer of carbon atoms in the honeycomb lattice structure, and has attracted much attention since its discovery.[1,2] It is an attractive platform for nanoscale electromechanical systems (NEMS)[3,4] due to its atomic thickness, low mass density, high stiffness and high surface area.[5,6] Several recent works have shown that graphene nanomechanical resonators (GNMR) are a promising candidate for ultrasensitive mass sensing and detection.[3,7] The quality (Q)-factors, and thus sensitivity to external perturbations like mass and pressure, are limited by both extrinsic and intrinsic energy dissipation mechanisms, including attachment induced energy loss,[8,9] nonlinear scattering mechanisms,[10] edge effects,[11] the effective strain mechanism[12] and thermalization due to nonlinear mode coupling.[13]

The interplay between graphene and adsorbates has been investigated in many works. It was experimentally shown that pristine graphene sheets are impermeable to standard gases, including helium.[4,14] The adsorption of helium atoms on graphene has also discussed,[15–17] while Jiang *et al.* studied the adsorption of metal atoms on the Q-factors of graphene resonators.[12] Very recently, an experiment showed that metal atoms can be used as molecular valves to control the gas flux through pores in monolayer graphene.[18] However, an important issue that has not been investigated is whether it is possible to self-assemble adsorbates on the graphene surface into different types of nanostructures.

In this letter, we report classical molecular dynamics (MD) simulations for the self-assembly of water molecules on the surface of graphene nanoresonators. In doing so, we draw inspiration from the classical macroscale Chladni plate resonators, in which higher order resonant modes are used to self-assemble adsorbates on the plate surface into different configurations.[19,20] We observe that the location for the self-assembly depends on the resonant frequency. Specifically, water molecules will assemble at the position with the maximum amplitude when the resonant frequency is lower than a critical frequency, which is determined by the interaction between graphene and water molecules. Otherwise, the assembly will take place at the position with minimum oscillation amplitude if the resonant frequency is higher than the critical frequency. We also analyze the hydrogen bonds for the water chains that are assembled by the graphene nanoresonators.

Our present work has revealed that it is possible for water molecules to assemble into water chains using graphene nanoresonators, which may have important implications for directed transport and ultra low friction-aided[21] advanced nanoscale conductance systems.[22] For example, Chen *et al.*[22] reported a water bridge under electric field can serve as a transport system, with potential applications in drug delivery. Water chains have also been created through confinement in

[a]*Division of Computational Mechanics, Ton Duc Thang University, Ho Chi Minh City, Vietnam. E-mail: timon.rabczuk@tdt.edu.vn*

[b]*Faculty of Civil Engineering, Ton Duc Thang University, Ho Chi Minh City, Vietnam*

[c]*Shanghai Institute of Applied Mathematics and Mechanics, Shanghai Key Laboratory of Mechanics in Energy Engineering, Shanghai University, Shanghai 200072, People's Republic of China*

[d]*Department of Mechanical Engineering, Boston University, Boston, Massachusetts 02215, USA. E-mail: parkhs@bu.edu*

[e]*Institute of Structural Mechanics, Bauhaus-University Weimar, 99423 Weimar, Germany*

[f]*College of Water Resources and Architectural Engineering, Northwest A&F University, 712100 Yangling, P. R. China*

carbon nanotubes. However, the radial size of the nanotubes limits the chain size, while also inducing water layering effects due to nanoconfinement, which may impact the fluid transport. Thus, assembling water chains *via* oscillating graphene surfaces may help to realize structurally flexible water channels in nanofluidics.

Fig. 1 shows the structure of the GNMR simulated in the present work, which is a monolayer and has dimensions 100 × 30 Å. All MD simulations were performed using the publicly available simulation code LAMMPS,[23] while the OVITO package was used for visualization.[24] The interaction among carbon atoms is described by the second generation Brenner (REBO-II)[25] potential, which is parameterized for carbon and/or hydrogen atoms. In the second-generation REBO force field, the total potential energy of a system is given by

$$E = \sum_i \sum_{j(>i)} \left[E_R(r_{ij}) - \bar{b}_{ij} E_A(r_{ij}) \right], \quad (1)$$

where E_R and E_A are the repulsive and attractive interactions, respectively. r_{ij} is the distance between two adjacent atoms i and j, and $\bar{b}_{ij}$ is a many-bond empirical bond-order term. The water molecules are described by the rigid SPC/E model.[26,27] The SHAKE algorithm implemented in LAMMPS was applied to freeze the high-frequency vibrations between oxygen and hydrogen atoms. The coupling between water molecules and graphene is represented by the interaction between oxygen atoms and graphene, which is described by the following Lennard-Jones (LJ) potential

$$U(r) = 4\varepsilon[(\sigma/r)^{12} - (\sigma/r)^6], \quad (2)$$

with parameters $\sigma_{C-O} = 3.19$ Å, $\varepsilon_{C-O} = 4.063$ meV.[28] The interaction among water molecules is also described by the LJ potential with $\sigma_{O-O} = 3.166$ Å, $\varepsilon_{O-O} = 6.737$ meV.[29] We find from the literature that the scanning electron microscope (SEM) is normally used to perform measurements on resonators,[30–32] which may help to study how water interacts with graphene nanoresonators. For the OH stretching, the potential energy associating with the OH stretching is one order higher than the interaction between water and graphene. Hence, the OH stretching motion is much weaker than the motion of the whole water molecular, so the water molecular is regarded as a rigid molecular by ignoring the OH stretching (which is a usual technique for the simulation of water). The standard Newton equations of motion are integrated in time using the velocity Verlet algorithm with a time step of 1 fs.

We first determine the resonant frequency for the GNMRs. Specifically, we actuate the resonant oscillation of the GNMR by adding a sine shaped velocity distribution to the z (out of plane) direction, *i.e.*, $v_z = v_0 \sin(2\pi x/L)$, in which L is the length in the x-direction. A small value $v_0 = 0.2$ Å ps^{-1} is used, so that nonlinear effects can be avoided. After the actuation, the GNMR is allowed to oscillate freely within the NVE (*i.e.*, the particles number N, the volume V and the energy E of the system are constant) ensemble. The resonant frequency $f_2\pi = 0.065$ THz is extracted from the trajectory of the kinetic/potential energy per atom. From elasticity theory, the frequency of the vibrational mode $\sin(n \times \pi x/L)$ with mode index n in the thin plate is proportional to n^2. Our numerical results show that $f = 0.016 \times n^2$ THz.

We now discuss the assembly of water molecules by using the resonant oscillation of GNMRs. The enforced oscillation is generated in the GNMRs by driving displacement $A \times \sin(\omega t) \sin(n \times \pi x/L)$ for carbon atoms, with $A = 8$ Å as the displacement amplitude. The angular frequency can be determined as $\omega = 2\pi f = 0.1 \times n^2$ THz. Water molecules are simulated within the NVT (*i.e.*, the particles number N, the volume V and the temperature T of the system are constant) ensemble. At the beginning of the simulations, 100 and 120 water molecules are randomly distributed on the surface of the GNMRs for mode index $n = 1$ and 2, respectively, as illustrated in Fig. 1. Fig. 2 shows the final stable structure at 300 K for mode indices $n = 1$ and 2, which shows obvious self-assembly of water molecules in both cases. As shown in Fig. 2, water molecules are assembled at $x = L/2$ for mode index $n = 1$, and at $x = L/4$ and $x = 3L/4$ for mode index $n = 2$, which indicates that water molecules are assembled at the positions with maximum amplitudes for mode indices $n = 1$ and 2.

The assembly of water molecules at positions with maximum oscillation amplitude can also be found in the graphene nanoresonator of circular (CGN) shape as shown in Fig. 3. For the CGN, the enforced oscillation is actuated in a similar way by pre-defining displacements $u_z = A \times \sin(2\pi ft)\sin(0.5\pi(1 - (r/R)))$ for the carbon atoms, where R is the radius of the graphene resonator and r represents the distance away from the center of the resonator. Fig. 3(a) shows the initial configuration of the

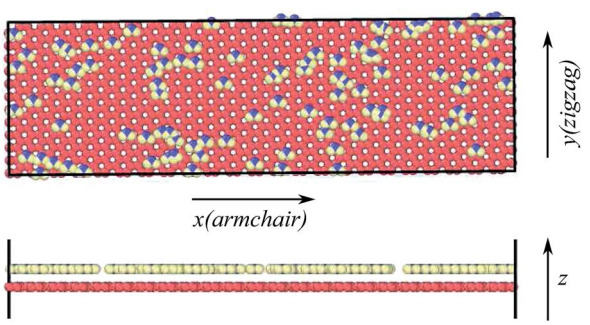

Fig. 1 Configuration for the GNMR. Water molecules are randomly distributed on the graphene sheet (red atoms) of dimensions 100 × 30 Å.

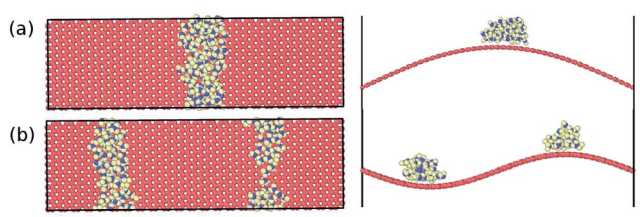

Fig. 2 Self-assembly of water molecules by GNMRs. The resonant oscillation corresponds to mode index $n = 1$ for panel (a) and $n = 2$ for panel (b). Water molecules are assembled at the positions with maximum amplitude.

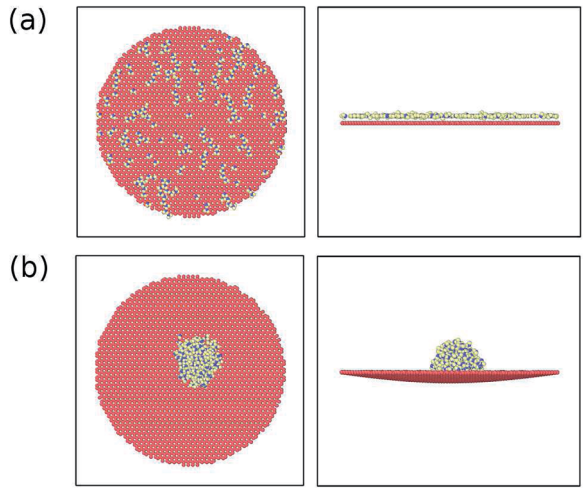

Fig. 3 (a) Initial configuration for the circular GNMR, with radius 50 Å. (b) Water molecules are assembled at the center of the CGN.

CGN of $R = 50$ Å and 196 water molecules. Fig. 3(b) shows that water molecules are assembled at the center of the CGN, which has the maximum oscillation amplitude.

To examine possible frequency effects on the self-assembly phenomenon, we performed a set of simulations with different frequencies for the resonant oscillation mode $n = 1$. More specifically, the intrinsic frequency for this mode is $f_\pi = 0.016$ THz. We simulated the self-assembly of water molecules for GNMRs oscillating at enforced frequencies of $3f_\pi$, $10f_\pi$, $30f_\pi$, $40f_\pi$, $50f_\pi$, $80f_\pi$ and $100f_\pi$. Fig. 4 shows the stable configuration of the system corresponding to frequencies $10f_\pi$, $30f_\pi$, $80f_\pi$ and $100f_\pi$. While the self-assembly of water molecules can be found in all cases, it clearly shows that the location for the water chains depend on the oscillation frequency. The assembly happens at the position with maximum oscillation amplitudes for lower oscillation frequencies $10f_\pi$ and $30f_\pi$, while the water chain is assembled at the two boundaries (with minimum oscillation amplitude) for higher oscillation frequencies $80f_\pi$ and $100f_\pi$. Fig. 5 summarizes the frequency dependence for the assembly position. There is a step-like jump at a critical frequency around $f_c = 35f_\pi$. Water molecules are assembled at

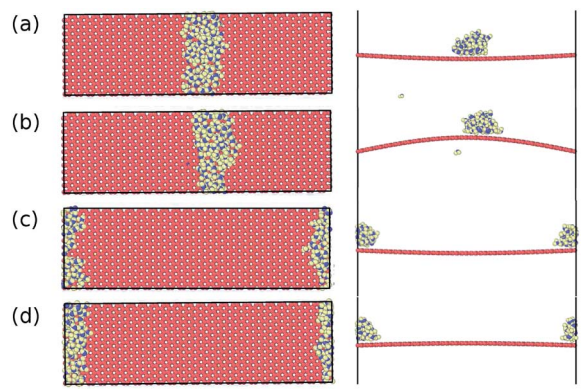

Fig. 4 Frequency effect on the self-assembly of water molecules with mode index $n = 1$, with 4 different frequencies ($10f_\pi$, $30f_\pi$, $80f_\pi$ and $100f_\pi$ for panels from (a) to (d)).

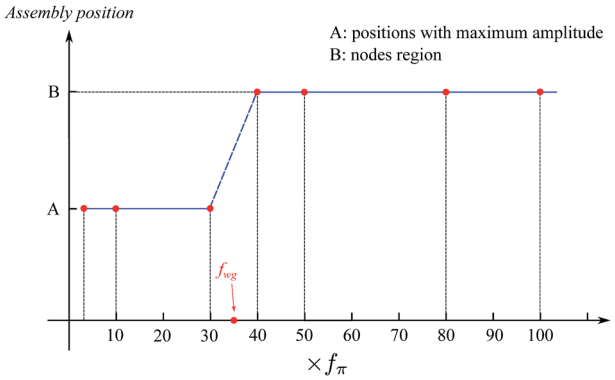

Fig. 5 Assembly position of water chains *versus* frequency for mode index $n = 1$.

the position with the maximum (minimum) oscillation amplitude, corresponding to frequencies lower (higher) than the critical frequency.

To understand the frequency dependent self-assembly, we explore two characteristic frequencies for the resonant oscillation process. The first frequency (f_g) is the resonant oscillation frequency for the GNMR, which has already been discussed. The second frequency (f_{wg}) characterizes the oscillation between the water clusters and graphene. The value of the second frequency is determined by the van der Waals interaction between water molecules and graphene. If the resonant frequency for graphene (f_g) is lower than the frequency f_{wg}, then water molecules are able to follow the resonant motion of the GNMR. As a result, water molecules are always connected to the GNMR through the van der Waals interactions during the oscillation process.

According to ref. 21, water molecules prefer to stay on surfaces with larger curvature. As a result, Fig. 6 shows that the water cluster slides down quickly to the position with maximum

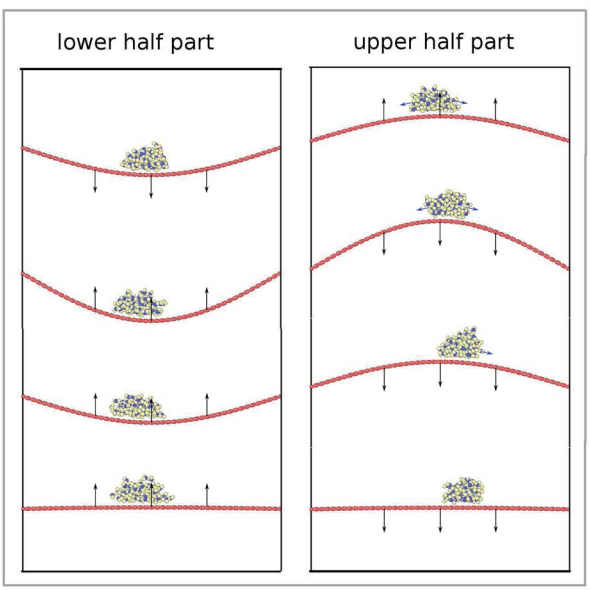

Fig. 6 The motion of a self-assembled water cluster during one oscillation cycle, with $f_g < f_{wg}$.

amplitude if the GNMR oscillation is below its equilibrium (flat) configuration. If the GNMR oscillation is above the flat configuration, the water cluster should move to the two ends, where the curvature is larger. It should be noted that the curvature is negative for the GNMR when it is above the equilibrium (flat) configuration as shown on the right part of Fig. 6. However, the sliding velocity of the water cluster is fairly small when the GNMR oscillation is above its equilibrium (flat) configuration. As a result, the water cluster oscillates around the middle of the GNMR with the maximum oscillation amplitude. However, if the resonant frequency for the GNMR (f_g) is higher than the frequency f_{wg}, then water molecules can escape from the van der Waals interactions from graphene and search for the most stable positions of the GNMR, leading to possible self-assembly of water chains at the nodal positions of the GNMR.

We now derive the frequency f_{wg} corresponding to the van der Waals interactions between water molecules and graphene. Assuming a small variation dr in the distance r, the retracting force constant can be obtained by

$$K = -\frac{\partial^2 U}{\partial r^2} = 0.023 \text{ eV Å}^{-2}. \quad (3)$$

The frequency for water molecules is

$$f_{wg} = \frac{1}{2\pi} \times \sqrt{\frac{K}{m}} \approx 0.567 \text{ THz}. \quad (4)$$

This analytic value for the critical frequency agrees quite well with the numerical results shown in Fig. 5, in which the numerical value for the critical frequency is about $35f_\pi \approx 0.56$ THz.

It is expected that the graphene liquid cell electron microscopy or the cryo-TEM technique can be applied to directly visualize the assembled water pattern on graphene film, which can provide direct experimental supports for our simulation results in the present work.

Quantifying the characteristics of the hydrogen (H)-bonding is useful for capturing important physical properties for water chains.[33–36] Therefore, we calculate the average number of H-bonds per water molecule in the water chains that are assembled for the different resonant frequencies. The H-bond is defined using the geometric criteria,[33] which states that a H-bond between two water molecules is formed if $r_{O\text{–}O} < 0.3$ nm and $\angle_{OOH} < 30°$. Fig. 7 shows that the highest value of the H-bonds number is about 3.3 for $100f_\pi$, which indicates that the water chain is spatially stable. This number is slightly smaller than 3.7 for bulk water due to the presence of surface effects on the formed water chains. The small value of the H-bonds number at the beginning of the assembly process is because many water molecules are spatially distributed at the beginning of the simulation. The number of the H-bonds increases and reaches a saturation value of 2.3, when a stable water chain is assembled. It is quite interesting that the saturation values for the number of the H-bond are almost the same for all water chains, which are assembled using different oscillation frequencies for the GNMR. This result implies similar structural properties for these water chains.

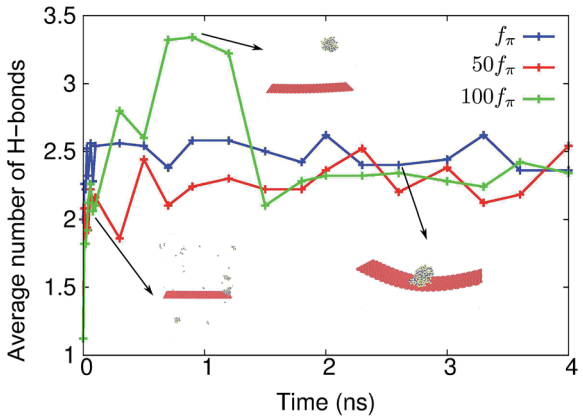

Fig. 7 Frequency effect on H-bonds.

In conclusion, we have demonstrated, using classical MD simulations, the possibility of creating self-assembled water nanostructures by using normal resonant mode shapes of graphene nanoresonators. In doing so, we have drawn inspiration from macroscale Chladni plate resonators, which are used to self-assemble shapes using higher order mode frequencies. We have uncovered that the location of the self-assembly can be controlled through the resonant frequency. Water molecules will assemble at the position with maximum amplitude if the resonant frequency is lower than a critical value. Otherwise, the assembly occurs at the nodes of the resonator, provided the resonant frequency is higher than the critical value. We provide an analytic formula for the critical resonant frequency based on the interaction between water molecules and graphene. Furthermore, we demonstrate that the water chains assembled by the graphene nanoresonators have some universal properties including a stable value for the number of hydrogen bonds.

Acknowledgements

The work is supported by the China Scholarship Council (CXW and CZ). JWJ is supported by the Recruitment Program of Global Youth Experts of China, the National Natural Science Foundation of China (NSFC) under Grant No. 11504225, and the start-up funding from Shanghai University. HSP acknowledges the support of the Mechanical Engineering department at Boston University.

References

1 K. S. Novoselov, A. K. Geim, S. V. Morozov, D. Jiang, Y. Z. S. V. Dubonos, I. V. Grigorieva and A. A. Firsov, *Science*, 2004, **306**, 666–669.
2 C. Berger, Z. Song, T. Li, X. Li, A. Y. Ogbazghi, R. Feng, Z. Dai, A. N. Marchenkov, E. H. Conrad, P. N. First and W. A. de Heer, *J. Phys. Chem. B*, 2004, **108**, 19912–19916.
3 J. S. Bunch, A. M. van der Zande, S. S. Verbridge, I. W. Frank, D. M. Tanenbaum, J. M. Parpia, H. G. Craighead and P. L. McEuen, *Science*, 2007, **315**, 490.

4 J. S. Bunch, S. S. Verbridge, J. S. Alden, A. M. van der Zande, J. M. Parpia, H. G. Craighead and P. L. McEuen, *Nano Lett.*, 2008, **8**, 2458–2462.
5 C. Lee, X. Wei, J. W. Kysar and J. Hone, *Science*, 2008, **321**, 385.
6 J.-W. Jiang, J.-S. Wang and B. Li, *Phys. Rev. B: Condens. Matter Mater. Phys.*, 2009, **80**, 113405.
7 B. Lassagne, D. Garcia-Sanchez, A. Aguasca and A. Bachtold, *Nano Lett.*, 2008, **8**, 3735–3738.
8 C. Seoánez, F. Guinea and A. H. C. Neto, *Phys. Rev. B: Condens. Matter Mater. Phys.*, 2007, **76**, 125427.
9 S. Y. Kim and H. S. Park, *Appl. Phys. Lett.*, 2009, **94**, 101918.
10 J. Atalaya, A. Isacsson and J. M. Kinaret, *Nano Lett.*, 2008, **8**, 4196–4200.
11 S. Y. Kim and H. S. Park, *Nano Lett.*, 2009, **9**, 969–974.
12 J.-W. Jiang, H. S. Park and T. Rabczuk, *Nanotechnology*, 2012, **23**, 475501.
13 D. Midtvedt, A. Croy, A. Isacsson, Z. Qi and H. S. Park, *Phys. Rev. Lett.*, 2014, **112**, 145503.
14 O. Leenaerts, B. Partoens and F. Peeters, *Appl. Phys. Lett.*, 2008, **93**, 193107.
15 M. Pierce and E. Manousakis, *Phys. Rev. Lett.*, 1998, **81**, 156.
16 Y. Kwon and D. M. Ceperley, *Phys. Rev. B: Condens. Matter Mater. Phys.*, 2012, **85**, 224501.
17 G. Derry, D. Wesner, W. Carlos and D. Frankl, *Surf. Sci.*, 1979, **87**, 629–642.
18 L. Wang, L. W. Drahushuk, L. Cantley, S. P. Koenig, X. Liu, J. Pellegrino, M. S. Strano and J. S. Bunch, *Nat. Nanotechnol.*, 2015, **10**, 785–790.
19 E. F. F. Chladni, *Entdeckungen über die Theorie des Klanges*, Zentralantiquariat der DDR, 1787.
20 T. D. Rossing, *Am. J. Phys.*, 1982, **50**, 271–274.
21 N. Wei, C. Lv and Z. Xu, *Langmuir*, 2014, **30**, 3572–3578.
22 J. Chen, C. Wang, N. Wei, R. Wan and Y. Gao, *Nanoscale*, 2016, **8**, 5676–5681.
23 LAMMPS, http://www.cs.sandia.gov/~sjplimp/lammps.html, 2012.
24 A. Stukowski, *Modell. Simul. Mater. Sci. Eng.*, 2010, **18**, 015012.
25 D. W. Brenner, O. A. Shenderova, J. A. Harrison, S. J. Stuart, B. Ni and S. B. Sinnott, *J. Phys.: Condens. Matter*, 2002, **14**, 783–802.
26 K. Falk, F. Sedlmeier, L. Joly, R. R. Netz and L. Bocquet, *Nano Lett.*, 2010, **10**, 4067–4073.
27 W. Xiong, J. Z. Liu, M. Ma, Z. Xu, J. Sheridan and Q. Zheng, *Phys. Rev. E: Stat., Nonlinear, Soft Matter Phys.*, 2011, **84**, 056329.
28 T. Werder, J. Walther, R. Jaffe, T. Halicioglu and P. Koumoutsakos, *J. Phys. Chem. B*, 2003, **107**, 1345–1352.
29 P. G. Kusalik, I. M. Svishchev, *et al.*, *Science*, 1994, **265**, 1219–1221.
30 J. S. Bunch, A. M. Van Der Zande, S. S. Verbridge, I. W. Frank, D. M. Tanenbaum, J. M. Parpia, H. G. Craighead and P. L. McEuen, *Science*, 2007, **315**, 490–493.
31 D. Garcia-Sanchez, A. M. van der Zande, A. S. Paulo, B. Lassagne, P. L. McEuen and A. Bachtold, *Nano Lett.*, 2008, **8**, 1399–1403.
32 D. Garcia-Sanchez, A. San Paulo, M. J. Esplandiu, F. Perez-Murano, L. Forró, A. Aguasca and A. Bachtold, *Phys. Rev. Lett.*, 2007, **99**, 085501.
33 S. Joseph and N. Aluru, *Nano Lett.*, 2008, **8**, 452–458.
34 A. Luzar, D. Chandler, *et al.*, *Nature*, 1996, **379**, 55–57.
35 G. Hummer, J. C. Rasaiah and J. P. Noworyta, *Nature*, 2001, **414**, 188–190.
36 N. Stahl and W. P. Jencks, *J. Am. Chem. Soc.*, 1986, **108**, 4196–4205.